Enhanced field-effect mobility in pentacene based organic thin-film transistors on polyacrylates

Jung-An Cheng, Chiao-Shun Chuang, Ming-Nung Chang, Yun-Chu Tsai, and Han-Ping D. Shieh

Citation: Journal of Applied Physics **105**, 064506 (2009); doi: 10.1063/1.3075873
View online: http://dx.doi.org/10.1063/1.3075873
View Table of Contents: http://scitation.aip.org/content/aip/journal/jap/105/6?ver=pdfcov
Published by the AIP Publishing

Enhanced field-effect mobility in pentacene based organic thin-film transistors on polyacrylates

Jung-An Cheng,[a] Chiao-Shun Chuang, Ming-Nung Chang, Yun-Chu Tsai, and Han-Ping D. Shieh
Department of Photonics and Display Institute, National Chiao Tung University, Hsinchu 30010, Taiwan, Republic of China

(Received 25 September 2008; accepted 20 December 2008; published online 19 March 2009)

We reported on organic thin-film transistors (OTFTs) with high dielectric constant polymer, poly(2,2,2-trifluoroethyl methacrylate) (PTFMA), as the gate dielectric. In top-contact OTFTs, the field-effect mobility was enhanced by applying a dielectric buffer layer poly(α-methylstyrene) to the bare PTFMA. After improving interfacial affinity within the active layer/dielectrics, deposited pentacene grain size and device performance were enhanced dramatically. The corresponding mobility, threshold voltage, and on/off current ratio were 0.70 $cm^2\ V^{-1}\ s^{-1}$, -10.5 V, and 5.4×10^5, respectively. The moderately improved interface also suppressed the hole-trapping effect, which led to less hysteresis and minimized threshold voltage shift. © *2009 American Institute of Physics*. [DOI: 10.1063/1.3075873]

I. INTRODUCTION

Polymeric dielectric materials are very attractive for organic thin-film transistor (OTFT) applications for all organic devices because they can often be formed by simply spin coating or printing at room temperature under ambient conditions.[1] Gate insulators in OTFTs also play a critical role because optimized selection of materials not only offers low operating voltage and gate leakage current but also often directly affects the mobility of charge carriers by modifying the orientation of organic semiconducting active materials.[2] Although polymeric insulators are still concerned for their low dielectric constant and high susceptibility to organic solvents, they are still considered as a preferred candidate mainly because of their interfacial compatibility with organic semiconductors that allows to easily control the chemical and physical properties of the dielectric surface and thus optimize device performance.[3–9]

Among various polymeric insulators, polymethylmethacrylate (PMMA) is of particular interest and is also a promising for a gate dielectric because it shows not only moderate output and transfer characteristics, high filed-effect mobility 0.241 $cm^2\ V^{-1}\ s^{-1}$,[10] and an excellent glasslike material in photonics.[11] PMMA also exhibits high potential as a substitute for brittle metal oxides as the gate dielectric in flexible OTFTs.[10,12] In addition, the solubility and thin-film properties of polyacrylates are tunable and dominated by varying the nature of ester substitutes. However, the low dielectric constant and film thickness dependence of PMMA lead to devices with a lower on/off current ratio, field-effect mobility, and severe hysteresis.[13,14]

In this study, we first reported OTFTs with high dielectric constant polymer, poly(2,2,2-trifluoroethyl methacrylate) (PTFMA), as the gate dielectric to enhance OTFTs performance. A buffer layer of poly(α-methystyrene) (PαMS) was utilized to modify the interfacial affinity between the PTFMA and pentacene. All of the output and transfer characteristics correlated with the test devices, including field-effect mobility (μ_{sat}), on/off current ratio (I_{on}/I_{off}), turn-on voltages (V_{on}), threshold voltages (V_{th}), and reliability will be examined.

II. EXPERIMENTAL

All of the materials used in this investigation are commercially available, and solvents were used without further purification. The molecular weight of commercial PαMS is 4000 g/mol. PTFMA was prepared according to Ref. 15, and its molecular weight and glass transition temperature were 30430 g/mol and 82.5 °C, respectively. Surface affinity of solid thin films was measured by using a Gardner contact angle detector.

The gate electrodes were made by photolithographic processing on an indium tin oxide (ITO) glass, and the ITO pattern had a dimension of 2.5×5.0 mm^2. The patterned ITO glass substrates for device fabrication were cleaned ultrasonically with detergent, de-ionized water, 2-propanol, and methanol, followed by UV-ozone pretreatment before use. For top-contact OTFT fabrication, PTFMA was dissolved in 1,2-dichloroethane, spin coated onto the ITO substrates, and dried in a vacuum oven. For the multilayered dielectric, PαMS was dissolved in toluene at 0.1 wt % and was spin coated onto the PTFMA solid thin film. Thereafter, pentacene was thermally deposited at 6×10^{-6} Torr ($\sim$0.3–0.4 Å s^{-1}) with a film thickness of 600 Å. Top-contact Au electrodes ($\sim$70 nm) were then subsequently deposited through a shadow mask. The channel length (L) and width (W) of the devices were 200 and 2000 μm, respectively. The film thickness and roughness were measured by an atomic force microscopy (AFM). The current-voltage (I-V) characteristics of the OTFTs were measured under inert gas by using a Keithley 4200 semiconductor parameter analyzer and an HP 4284 CV analyzer, respectively.

[a]Electronic mail: jacheng.ac89g@nctu.edu.tw.

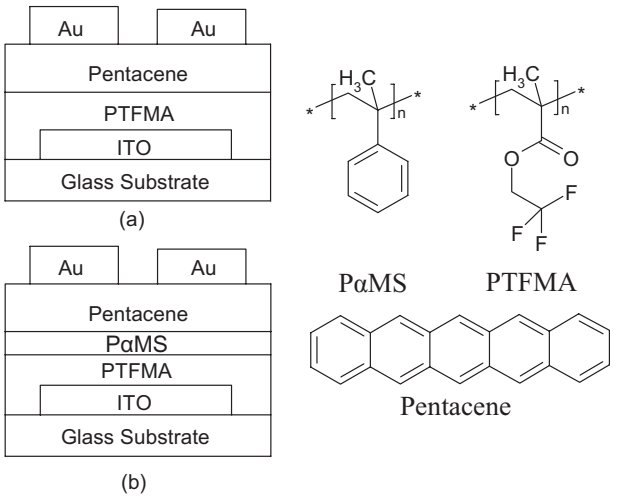

FIG. 1. Schematic structure of the OTFT devices with different dielectric layers: (a) pristine PTFAM and (b) PαMS/PTFMA.

III. RESULT AND DISCUSSION

To investigate the polymeric gate dielectrics on pentacene-based OTFTs, two kinds of devices were fabricated. The OTFT configuration and the chemical structures of dielectrics are depicted in Fig. 1. The dielectric thin-film properties are characterized and summarized in Table I. In the solubility test, it was found that PαMS was soluble in 1,2-dichloroethane and toluene, but PTFMA was insoluble in toluene. Therefore, to study the fabrication of two-layered dielectrics, PαMS dissolved in toluene at 0.1 wt % was spun onto PTFMA solid thin film. The thicknesses of PTFMA and PαMS were 592 and 10 nm, respectively. In the AFM measurement, a flat PαMS/PTFMA thin film with pinhole free surface was observed, and the surface roughnesses of pristine PTFMA and PαMS/PTFMA were 0.44 and 0.51 nm, respectively. Due to the coated PαMS buffer layer, the surface affinity of the treated PTFMA thin film became more hydrophilic, and the corresponding contact angle and surface energy were modified from 95.1° and 24.13 mJ/m^2 to 84.0° and 31.12 mJ/m^2, respectively.

TABLE I. Gate dielectric thin-film surface characteristics.

Dielectric material	Surface roughness (R_a) (nm)	Contact angle (deg)	Dielectric constant (k)	SFE (mJ m^{-2})[a]
PTFMA	0.44	95.1	6.0	24.13
PαMS [b]	0.51	84.0	2.5	31.12

[a]The contact angle and the SFE of pentacene thin film were measured and estimated at 88.7° and 28.80 mJ m^{-2}, respectively.
[b]PαMS was spun onto the PTFMA solid thin film.

The output characteristics (I_{DS} versus V_{DS}) as a function of gate voltages (V_{GS}) for pentacene TFTs using different gate dielectrics are plotted in Figs. 2(a) and 2(b), respectively. Both devices showed saturated and linear characteristics under different V_{GS} bias. The I_{DS}-V_{DS} output characteristics showed a *p*-channel accumulation type field-effect transistor.

The transfer characteristics of the test devices were measured in the saturation region ($|V_{DS}|=30\ \text{V} \geq |V_{GS}-V_{th}|$), and the representative transfer plots are shown in Figs. 2(c) and

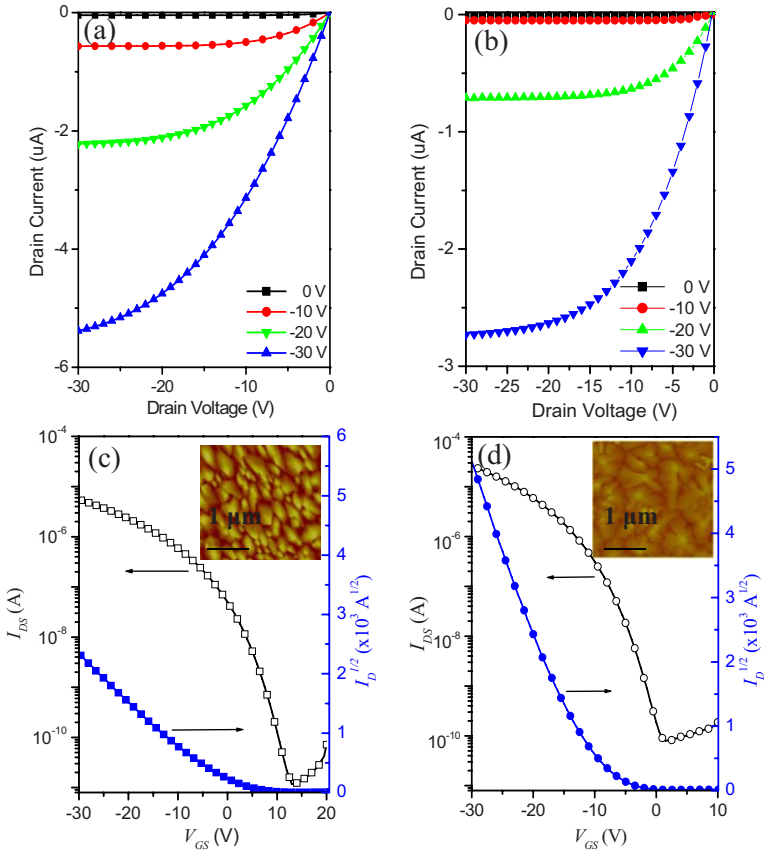

FIG. 2. (Color online) Electrical properties of OTFTs with different gate dielectrics. Output characteristics: (a) pristine PTFMA; (b) PTFMA coated with PαMS. Transfer characteristics: (c) pristine PTFMA; (d) PTFMA coated with PαMS. The gate voltage is swept at a constant drain-source voltage $V_{DS}=-30$ V. Inset: AFM images (3×3 μm^2) of pentacene film topography grown on polymeric dielectrics.

TABLE II. Electrical performance parameters for OTFTs with different gate dielectrics (note: the side-chain groups are for gate dielectrics).

Insulators	Filed-effect mobility (μ_{sat}) ($cm^2\ V^{-1}\ s^{-1}$)	On/off current ratio (I_{on}/I_{off})	I_{off} current (A)	Turn-on voltage (V_{on}) (V)	Subthreshold swing (V/decade)	Threshold voltage (V_T) (V)	Dipole moment (D)[a]
PTFMA	0.10	4.7×10^5	1.18×10^{-11}	12.0	2.24	−2.20	2.54[b]
PαMS/PTFMA	0.70	5.4×10^5	1.86×10^{-10}	1.8	2.60	−10.5	0[c]

[a]Reference 23.
[b]Fluoroester group ($-C(O)OC_2CF_3$).
[c]Phenyl group ($-C_6H_5$).

2(d), respectively. The source-drain current $|I_{DS}|$ in a logarithmic scale was shown against the gate voltage V_G at a constant source-drain voltage of $V_{DS}=-30$ V. For devices with different gate dielectrics, field-effect mobility (μ_{sat}) and threshold voltage were measured from these current-voltage characteristics in the saturated region using a linear fit to plot the square root of the drain current I_{DS} as a function of gate voltage V_G.[16] All of the parameters related to the transfer characteristics were extracted and summarized in Table II. The field-effect mobility (μ_{sat}) and the on/off current ratio (I_{on}/I_{off}) for a pristine PTFMA device were 0.10 $cm^2\ V^{-1}\ s^{-1}$ and a magnitude of five orders, respectively. After PαMS modification with a buffer layer at a thickness of 10 nm, the I_{on}/I_{off} value was close to that of the pristine PTFMA device, but the field-effect mobility (μ_{sat}) was dramatically enhanced to 0.70 $cm^2\ V^{-1}\ s^{-1}$, which was 2.9 times higher than that of optimized PMMA devices.[10] This improvement may be due to a reduction in interface trap densities resulting from moderate adjustment in the pentacene attributes to the moderate surface free energy (SFE) after treatment. After inspecting the topology of pentacene thin films inserted in Figs. 2(c) and 2(d), we found that the grain size on the modified surface with PαMS, shown in Fig. 2(d), was larger than that of pristine PTFMA revealed in Fig. 2(c). The grain sizes were measured at 0.25–0.70 and 0.81–1.51 nm for PTFMA and PαMS, respectively. This fact was attributed to the PαMS buffer layer, which enhanced the SFE to 31.12 mJ/m^2 from that of pristine PTFMA at 24.13 mJ/m^2, as a result the number of nucleation sites decreased, which also resulted in a grain boundary reduction. Accordingly, hole-trapping sites were reduced in PαMS/PTFMA, which led to a higher field-effect mobility of 0.70 $cm^2\ V^{-1}\ s^{-1}$. Similar OTFT characteristics with double-layered dielectrics were also demonstrated by Stadlober *et al.*[17] Although Müller *et al.*[18] also presented an OTFT with two-layer gate dielectrics and reduced its operation voltage, the corresponding transfer characteristics showed the poor field-effect mobility.

Through a linear fit for $I_{DS}^{1/2}$-V_G curves, we were able to estimate V_{th} and μ_{sat} in the saturation region. Thus, the $I_{DS}^{1/2}$-V_G relations of the devices are plotted in Figs. 2(c) and 2(d), respectively. Of particular interest was the change in V_{th} and V_{on} on different dielectric surfaces. To the best of our knowledge, no conclusive theory has been proposed to explain the extraordinary properties of the PαMS surface treatment. Although the theory proposed by Chua *et al.*[19] may provide an explanation, PαMS does not present electron-tapping sites, such as $-CF_3$ and ester groups, to the organic semiconductor, this may lead to increased electrical behavior. Moreover, in the case of the PαMS-treated sample, V_{on} is close to zero voltage, which leads to a more negative V_{th} at −10.5 V. The difference between V_{th} and V_{on} is smaller in the case of PαMS-treated OTFTs ($\Delta V=12.0$ V) than that of pristine PTFMA OTFT ($\Delta V=14.4$ V), which can be accounted for by a smaller amount of hole traps in the *p*-type OTFT.[20] A positive onset voltage, as observed in the PTFMA OTFT, is usually attributed to the presence of fixed negative charges, presumably in the form of trapped electrons at the interface between pentacene and the gate dielectric. The near-zero onset voltage of the PαMS-treated OTFTs suggested that there are almost no electrons trapped at the interface between PαMS and pentacene film.[19]

On the other hand, the observed V_{th} and V_{on} shift correlates to the electron affinity of the polymeric insulator end groups. The dipole structures in PTFMA synchronously form a built-in dipole-dipole field, and the induced field is equivalent to a gate voltage applied in the transistor channel. The electronegativity of the terminal functional group ($-CF_3$) on PTFMA influences the charge distribution within the gate insulator and pentacene, and can lead to the formation of an electric dipole within the dielectric/pentacene interface, as shown in Fig. 3(a).[21] As a result, the charge density at the insulator-organic semiconductor interface has been intrinsically organized to affect device performance dramatically. When pentacene is deposited onto a dielectric layer without the dipole effect, i.e., the device shown in Fig. 1(a), the vacuum levels are aligned and no bending of the highest occupied molecular orbital (HOMO) and lowest unoccupied molecular orbital (LUMO) levels occurs, as shown in Fig.

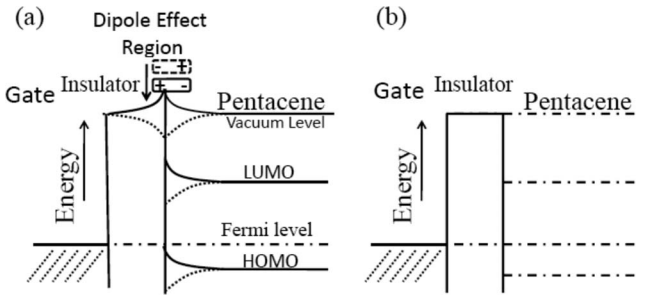

FIG. 3. Schematic energy level diagram for illustrating the interface between gate insulators and pentacene in top-contact devices: (a) with and (b) without dipole effect on the gate dielectric/pentacene interface. The "+" and "−" denote the hole and electron, respectively.

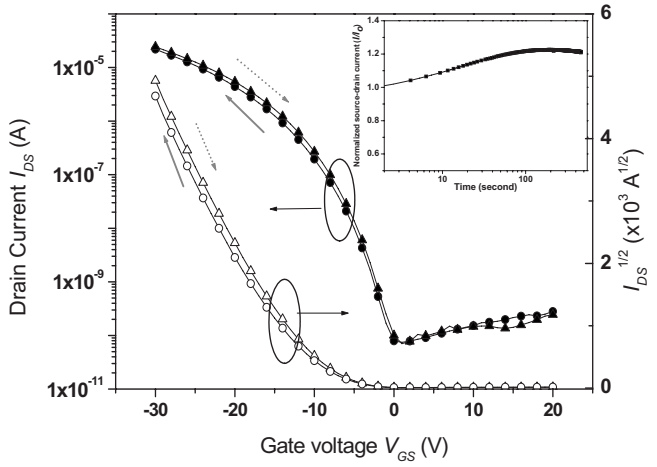

FIG. 4. Hysteresis in transfer characteristics of the PαMS/PTFMA based OTFT. The solid arrow and the dotted arrow indicate the forward and backward sweep, respectively. The gate voltage was swept at a constant drain-source and gate voltage: $V_{GS}=V_{DS}=-30$ V. Inset: the normalized source-drain current (I/I_0) degradation as a function of time after stress.

3(b). When a negative gate voltage is applied, the Fermi level of the gate electrode shifts toward higher (electron) energies. Part of the applied gate voltage is dropped across the gate insulator, and since the band alignment of the HOMO and LUMO levels is fixed with respect to vacuum level, the remaining gate voltage bends HOMO and LUMO levels. As a result, mobile charge carriers can be accumulated in the conducting channel. For a PTFMA dielectric with a permanent dipole field inserted between the gate electrode and the pentacene, as shown in Fig. 3(a), the dipole field of the polymeric insulator modifies the surface potential which has the same effect as applying a (negative) gate voltage. For a *p*-type OTFT, therefore, V_{th} and V_{on} will shift to the more positive region when a polymer with high dipole moment is used as a gate dielectric layer.

For general organic circuit applications such as radio-frequency identification transponders, the OTFT devices were essential of minimized hysteresis because the threshold voltage (V_{th}) shift caused by the hysteresis behavior may result in unpredictable circuit operation. Therefore, a practical dielectric was required to have lower hysteresis.[22] In the reliability test, the transfer characteristics and voltage bias stress were measured and plotted in Fig. 4. The OTFT device based on PαMS/PTFMA showed less hysteresis ($\Delta V_{GS}=-0.25$ V) during forward and backward sweeps, which could be attributed to the PαMS. Buffer layer retarded the change in surface polarity of PTFMA. The inset is the normalized source-drain current (I/I_0) degradation as a function of time after stress test. Obviously, the I/I_0 ratio initially increased with stress time under a constant bias, and saturated at 1.20 at 500 s. In comparison, the I/I_0 ratio for the PTFMA based OTFT device initially decreased with stress time, and saturated at 0.86 at 340 s. Furthermore, hysteresis was 0.62 V at $V_{GS}=-30$ V for the PαMS/PTFMA device, which is smaller than that of pristine PTFMA estimated at 0.84 V.

IV. CONCLUSION

We have demonstrated top-contact OTFTs with PTFMA as a gate dielectric, which significantly enhanced the performance by depositing a buffer layer of PαMS onto the bare PTFMA. Via the simplified surface treatment with pinhole free morphology, we cannot only enhance the pentacene grain size to achieve an OTFT high mobility, but also eliminate the built-in electric filed in the bottom gate dielectric to minimize the threshold voltage shift and hysteresis. Accordingly, our research on bilayered polymeric gate dielectrics with moderate permittivity and low defect could provide an alternative for fabricating flexible and large area substrates with full solution process, such as roll-to-roll and inkjet printing technology.

ACKNOWLEDGMENTS

This work was supported by the MOE ATU Program "Aim for the Top University" No. 97W802 and the National Science Council of Taiwan under Contract No. NSC96-2628-E009-021-MY3.

[1] A. Facchetti, M.-H. Yoon, and T. J. Marks, Adv. Mater. (Weinheim, Ger.) **17**, 1705 (2005).
[2] K. Puntambekar, J. Dong, G. Haugstad, and C. D. Frisbie, Adv. Funct. Mater. **16**, 879 (2006).
[3] H. C. Yang, S. H. Kim, L. Yang, S. Y. Yang, and C. E. Park, Adv. Mater. (Weinheim, Ger.) **19**, 2868 (2007).
[4] C. Kim, A. Facchetti, and T. J. Marks, Adv. Mater. (Weinheim, Ger.) **19**, 2561 (2007).
[5] G. Nunes, Jr., S. G. Zane, and J. S. Meth, J. Appl. Phys. **98**, 104503 (2005).
[6] S. Pratontep, F. Nuesch, L. Zuppiroli, and M. Brinkmann, Phys. Rev. B **72**, 085211 (2005).
[7] W. S. Hu, Y. T. Tao, Y. J. Hsu, D. H. Wei, and Y. S. Wu, Langmuir **21**, 2260 (2005).
[8] Y. Zheng, D. C. Qi, N. Chandrasekhar, X. Y. Gao, C. Troadec, and A. T. S. Wee, Langmuir **23**, 8336 (2007).
[9] R. Ruiz, D. Choudgary, B. Nickel, T. Toccoli, K.-C. Chang, A. C. Mayer, P. Clancy, J. M. Blakely, R. L. Headrick, S. Iannotta, and G. G. Malliaras, Chem. Mater. **16**, 4497 (2004).
[10] T.-S. Huang, Y.-K. Su, and P.-C. Wang, Appl. Phys. Lett. **91**, 092116 (2007).
[11] D. L. Keyes, R. R. Lamonte, D. McNally, and M. Bitritto, Photonics Spectra **35**, 131 (2001).
[12] K. Müller, I. Paloumpa, K. Henkel, and D. Schmeißer, Mater. Sci. Eng., C **26**, 1028 (2006).
[13] C.-S. Chuang, S.-T. Tsai, Y.-S. Lin, F.-C. Chen, and H.-P. D. Shieh, Jpn. J. Appl. Phys., Part 2 **46**, L1197 (2007).
[14] T. S. Huang, Y. K. Su, and P. C. Wang, Jpn. J. Appl. Phys. **47**, 3185 (2008).
[15] W. Liu, K. Tang, Y. Guo, Y. Koike, and Y. Okamoto, J. Fluorine Chem. **123**, 147 (2003).
[16] S. M. Sze, *Semiconductor Devices* (Wiley, New York, 1985), Chap. 5.
[17] B. Stadlober, M. Zirkl, M. Beutl, and G. Leising, Appl. Phys. Lett. **86**, 242902 (2005).
[18] K. Müller, I. Paloumpa, K. Henkel, and D. Schmeisser, J. Appl. Phys. **98**, 056104 (2005).
[19] L.-L. Chua, J. Zaumseil, J.-F. Chang, E. C.-W. Ou, P. K.-H. Ho, H. Sirringhaus, and R. H. Friend, Nature (London) **434**, 194 (2005).
[20] G. Horowitz and P. Delannoy, J. Appl. Phys. **70**, 469 (1991).
[21] I. H. Campbell, S. Rubin, T. A. Zawodzinski, J. D. Kress, R. L. Martin, D. L. Smith, N. N. Barashkov, and J. P. Ferraris, Phys. Rev. B **54**, R14321 (1996).
[22] P. Balk, Adv. Mater. (Weinheim, Ger.) **7**, 703 (1995).
[23] *Handbook of Organic Chemistry*, 2nd ed., edited by G. W. Gokel (McGraw-Hill, New York, 2004).